

Article

# Geochemical Characterization, Geochronology, and Geodynamic Implications of Grenville Rare Earths Bearing Syenites, Haut-Saint-Maurice, QC, Canada

Gabriel Côté<sup>1</sup>, Abdelali Moukhsil<sup>2</sup> , Marc Constantin<sup>1,\*</sup> and Jean David<sup>3</sup>

<sup>1</sup> Department of Geology and Geological Engineering, Faculty of Science and Engineering, Université Laval, Quebec, QC G1V 0A6, Canada; gabriel.cote.12@ulaval.ca

<sup>2</sup> Ministère de l'Énergie et des Ressources Naturelles, Quebec City, QC G1H 6R1, Canada; abdelali.moukhsil@mern.gouv.qc.ca

<sup>3</sup> Stable Isotope Geochemistry Laboratory (GEOTOP), Montreal, QC H2X 3Y7, Canada; jean.david@mern.gouv.qc.ca

\* Correspondence: marc.constantin@ggl.ulaval.ca

Received: 6 June 2018; Accepted: 26 July 2018; Published: 5 August 2018



**Abstract:** The syenites in the western part of the Grenville Province in Quebec have been known since the 1990s, but few studies have been carried out on them. Over the last three years, a mapping project carried out by the Ministère de l'Énergie et des Ressources naturelles has revealed the presence of several rare earth element (REE)-bearing syenitic intrusions in this area. In this paper, we present a geodynamic model for their formation based on geochemical, thermobarometric, and geochronological data. The intrusions were emplaced between 1038 +15/−13 Ma and 1009 ± 3 Ma. The syenites can be divided into two groups: (1) an older, REE-bearing group associated with a volcanic arc and (2) a younger group with lower REE contents associated with an anorogenic event. Formation temperatures were between 898 and 1005 °C, and pressures were between 2 and 10 kbar. This model involving two intrusive periods is in conflict with the model of a large, hot, long-duration collisional orogen proposed by Rivers et al. (2009) but is consistent with more recent studies.

**Keywords:** Grenville; syenite; REE

## 1. Introduction

Rare earth element (REE) deposits in the Quebec part of the Grenville Province are related either to pegmatitic granitic dykes [1] or to alkaline intrusions [2–6], and they are often rich in light rare earth elements (LREEs). LREEs are used, for example, in the construction of strong permanent magnets employed in the manufacturing of miniature electronic devices and wind turbines [7]. Since 2010, Chinese authorities have reduced REE exports, and this has resulted in either relocalization of the industries using REE in China or finding new REE sources [8]. Because of the critical need for new sources, the Grenville Province has become very attractive for this type of deposit.

A number of alkaline intrusions were studied in the course of a recent regional mapping program carried out by the Ministère de l'Énergie et des Ressources naturelles (MERN) in the Mont-Laurier area of Québec [2–4]. These intrusions occur as dykes and small, subcircular bodies that cut all other units. They are generally surrounded by a shear zone.

A large body of geochronological data on alkaline intrusions in the Quebec part of the Grenville Province is available ([5] (Kipawa area), [9] (Lesueur intrusion), [10] (Kensington-Skootamatta area), and [2–4]). These studies have provided ages for the syenites between 1089 and 1000 Ma, a range that includes the Ottawa and Rigolet orogenic pulses, as defined by Rivers et al. [11].

In this paper, we separate the intrusions into groups that allow a better understanding of the formation processes of the syenites and their associated REE deposits. We propose a geodynamic model for their formation, and we compare it with the earlier model by Augland et al. [12]. Separation of the syenites into groups is based on their chemistry, mineralogy, and calculated pressures (P) and temperatures (T) of crystallization.

### 1.1. Regional Geology

The study area is located in the Allochthonous Belt of the Grenville Province, as defined by Rivers et al. [13]. The rocks of the area are of Paleoproterozoic to Mesoproterozoic age and were formed during a succession of orogenic and extensional periods. Gower and Krogh divided the collisional and extensional events in the Canadian part of the Grenville Province into three phases [14]: (1) the pre-Labradorian (>1710 Ma) and Labradorian (1710–1600 Ma) period, (2) the period between 1600 and 1230 Ma, and (3) the period corresponding to a continent-continent collision (1230 to 985 Ma). Rivers et al. (2012) [11] also considered the issue of the ages of collision and extension in eastern Grenville using LITHOPROBE (A Canadian national geoscience project aiming to research and map the lithosphere structure and composition) data. They concluded that a continent-continent collision occurred between 1090 to 980 Ma, and they separated the orogenic period into two phases: (1) the Ottawa phase (1090 to 1020 Ma), during which rocks in the Allochthonous Belt were characterized by a granulitic facies metamorphism [15] and (2) the Rigolet phase (1010 to 980 Ma), characterized by amphibolite facies metamorphism.

The area of this study (Figure 1) is located in the northern part of the Central Metasedimentary Belt (CMB) in Quebec, Canada [16]. In this region, Currie (1976), Corriveau (1990), and Blein et al. (2003) defined an 800-km-long nepheline syenite belt formed of small intrusions and subcircular plutons, concordant or not with surrounding rocks located in the eastern part of Ontario and the west of Quebec [16–18]. The emplacement of these rocks is interpreted to have occurred in an active subduction zone [18]. With crystallization ages between 1089 and 1076 Ma [19].

### 1.2. Local Geology

In our study area (Figure 2), Pinwarian rocks of the Hibbard Plutonic Suite ( $1503 \pm 35$  Ma,  $1468 \pm 7$  Ma; Moukhsil et al. [2]) intrude Labradorian rocks of the Dugré Plutonic Suite ( $1674 \pm 15$  Ma; [2]). Elsonian metasedimentary rocks occur in kilometers tectonic enclave scattered across the territory (Wabash Metasedimentary Complex  $<1204 \pm 12$  Ma). Igneous activity ended with the Late-Grenvillian, K-rich dykes and small, intrusions of the Roc Igneous Suite and finally the subject of this paper, the subcircular syenitic intrusions (1040–1004 Ma, [2,4]). Moreover, to better define the timing of the late magmatism, new radiometric ages have been carried out, that will be presented later.

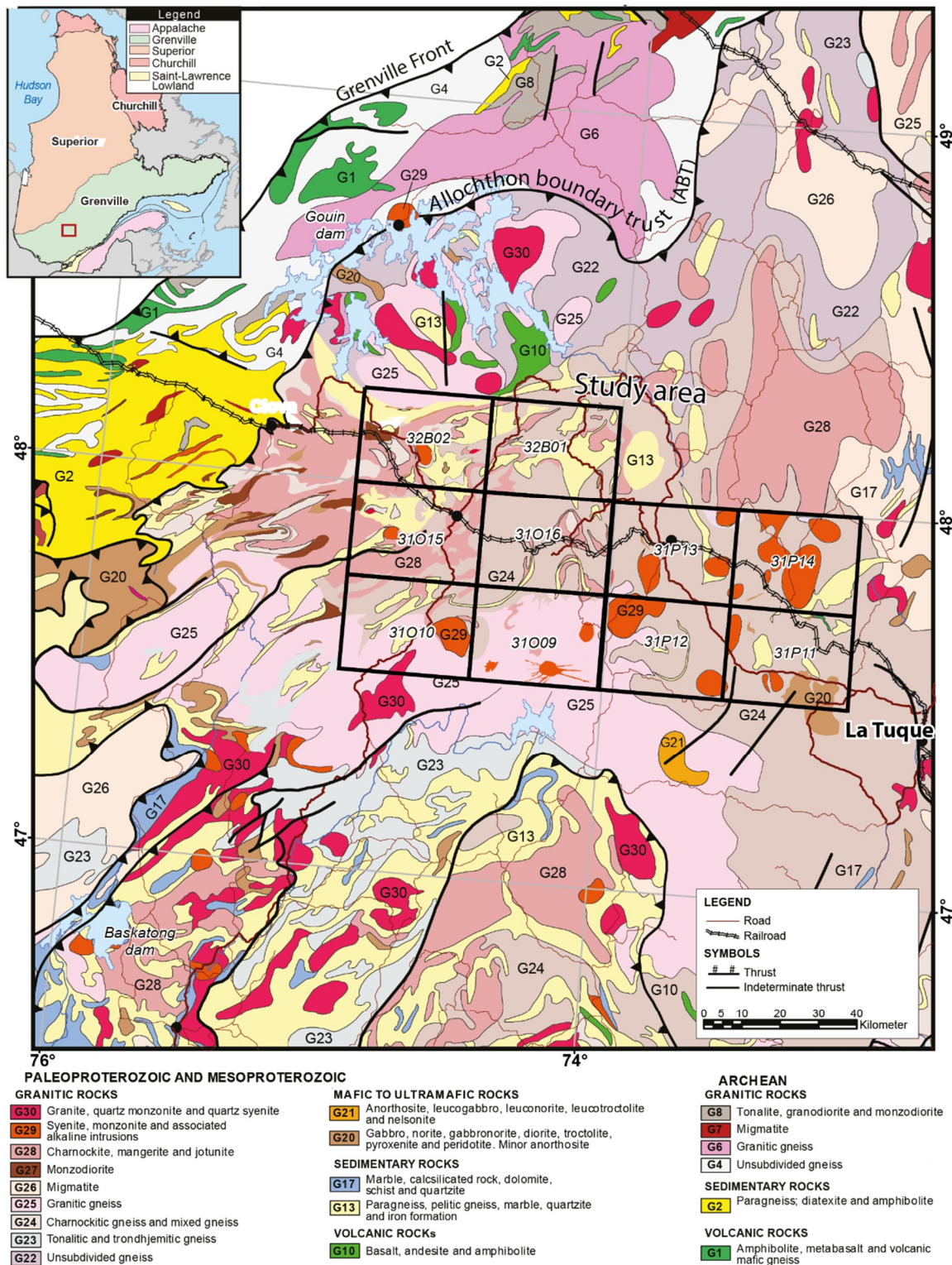


**Figure 1.** Regional geology showing the study area located in the allochthon part of the Grenville Province. This figure shows the position of the study area relative to the allochthon boundary trust and the central metasedimentary belt in the south. The alkaline intrusion corresponds to the G29 red-orange intrusion.

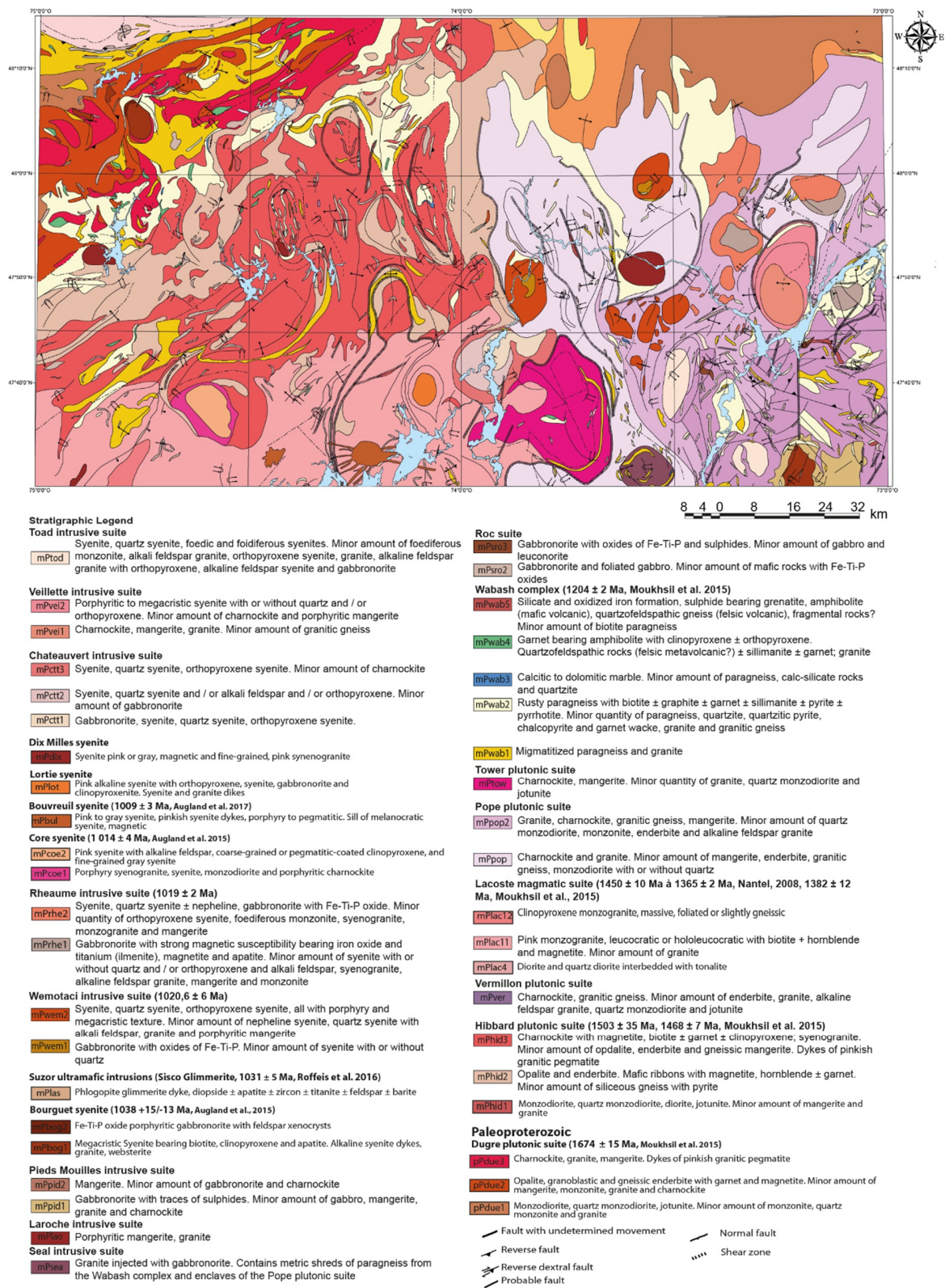


**Figure 2.** Local detailed geology showing the study area in the Wemotaci and Parent regions, Quebec, Canada. The mapping of this part was done in 2014 and 2016 [2,4].

### 1.2.1. Wemotaci Intrusive Suite

The Wemotaci Intrusive Suite is composed of two subunits (1) gabbro-norite with minor syenite, and (2) syenite and quartz-bearing syenite, locally with orthopyroxene (Figure 3a). The main lithology is a pink syenite, which is foliated near the border of the intrusion and massive in the center. The main minerals are potassic feldspar, as tabular phenocrysts 1–2.5 cm long, plagioclase, and magnetite. Orthopyroxene, clinopyroxene, biotite, hornblende, and apatite are accessory minerals. Orthopyroxene-bearing syenite is porphyritic, medium-grained, and pinkish (on fresh surface), but greenish where injected by dikes. This rock is composed of K-feldspar phenocrysts, deformed quartz, and garnet. Quartz-bearing syenite is porphyritic, medium-grained and is composed of K-feldspar phenocrysts 1–1.5 cm long, quartz, orthopyroxene, clinopyroxene, hornblende, biotite and zircon, and apatite as accessory minerals.

### 1.2.2. Veillette Intrusive Suite

This suite is composed of two assemblages: (1) charnockite–mangerite–granite and (2) syenite–quartz-bearing syenite (locally bearing orthopyroxene)–charnockite–mangerite. Syenite is porphyritic to megacrystic, massive, and green on fresh surfaces. It contains biotite and garnet as accessory minerals. K-feldspar phenocrysts are around 4.5 cm long and constitute 45% of the rock. Quartz-bearing syenite contains perthitic K-feldspar and orthopyroxene that is almost completely replaced by hornblende. Mangerite and charnockite are of minor importance in this unit.

### 1.2.3. Chateaufort Intrusive Suite

The Chateaufort Intrusive Suite is composed of three assemblages: (1) gabbro-norite–syenite–quartz bearing syenite–orthopyroxene-bearing syenite, (2) syenite–quartz syenite–K-feldspar syenite–orthopyroxene-bearing syenite–gabbro-norite (minor), and (3) syenite–quartz syenite–, orthopyroxene-bearing syenite–charnockite (minor). All types of syenite are medium grained, foliated, magnetic, and locally porphyritic in K-feldspar. In thin section, the syenites contain up to 30% K-feldspar phenocrysts. Where present, quartz and orthopyroxene occur as large crystals associated with hornblende and can exceed 10% in abundance.

### 1.2.4. Rheaume Intrusive Suite

The Rheaume Intrusive Suite (Figure 3b) is composed of two assemblages: (1) magnetite- and apatite-bearing gabbro-norite, with minor syenite, quartz syenite, syenogranite, K-feldspar granite, mangerite, and monzonite, and (2) syenite–quartz syenite–magnetite- and apatite-bearing gabbro-norite. Syenite is grey or pink and contains K-feldspar phenocrysts. Nepheline occurs locally as an accessory mineral. Syenogranite is pink and medium grained. All lithofacies in this unit contain biotite, clinopyroxene, and magnetite. Orthopyroxene-bearing syenite is grey to pink on fresh surface and is medium grained. Biotite and hornblende occur near orthopyroxene, plagioclase is tabular, and apatite and zircon are accessory minerals.

### 1.2.5. Toad Intrusive Suite

The Toad Intrusive Suite is composed of grey and pink syenite, K-feldspar syenite, foid-bearing syenite, and foid-bearing monzosyenite. Grey syenite is fine grained and grey on weathered surfaces. Pink syenite dikes are medium grained and cut grey syenite. Such injections are rich in biotite (up to 15%), are massive (except in deformation zones), and exhibit magmatic structures. In thin section, both types of syenite contain K-feldspar, albite, magnetite, biotite, clinopyroxene, hornblende, apatite, zircon, and locally orthopyroxene. Microcline is the dominant feldspar. K-feldspar syenite is locally pegmatitic, contains at least 2% biotite, and locally contains quartz or orthopyroxene or nepheline. Foid-bearing monzonite is grey on fresh and weathered surfaces. It forms enclaves, 20–50 cm in diameter, in grey syenite. Grey syenite contains up to 10% biotite and titanite, with apatite

and zircon as accessory minerals. Foid-bearing monzosyenite is medium grained and is grey on fresh surfaces. It is composed of clinopyroxene, biotite, amphibole, K-feldspar, plagioclase, magnetite and nepheline. Electron microprobe (CAMECA SX-100, CAMECA, Gennevilliers, France) analyses show that plagioclase is mainly albite and contains orthopyroxene and K-feldspar inclusions. These lithofacies also contain allanite (Ce-type, [3]) and parisite (a LREE-bearing Ca-fluocarbonate).

#### 1.2.6. Dix Milles Syenite

This unit consists of three small intrusions composed of grey and pink syenite. Both lithofacies are medium grained and massive. Both contain K-feldspar, amphibole, clinopyroxene, apatite, ilmenite, and accessory orthopyroxene. Syenogranite associated with the syenite is composed of K-feldspar, quartz, plagioclase, ilmenite, apatite, and accessory hornblende.

#### 1.2.7. Lortie Syenite

This unit is composed of pink, medium-grained syenite. It consists of K-feldspar, orthopyroxene, plagioclase, hornblende, magnetite, and biotite, along with accessory apatite, ilmenite, and clinopyroxene. Clinopyroxenite and gabbro-norite are associated with the syenite. A few granitic dikes cut the intrusion.

#### 1.2.8. Core Syenite

The Core Syenite, dated to  $1014 \pm 4$  Ma by [12] (Figure 3c), is composed of two assemblages: (1) porphyritic syenogranite–syenite–monzodiorite–porphyritic charnockite and (2) pink K-feldspar syenite–grey syenite. The porphyritic syenogranite is the dominant rock of the group 1. It is pink on fresh surfaces and beige on weathered surfaces, coarse grained, and composed of K-feldspar, quartz, magnetite, biotite, and amphibole, with apatite, ilmenite, titanite, and zircon as accessory minerals. K-feldspar syenite and grey syenite are coarse grained and show magma-mingling textures [2]. The main minerals are K-feldspar, albite, magnetite, clinopyroxene, biotite, apatite, hornblende and orthopyroxene, and ilmenite and titanite are accessory phases.

#### 1.2.9. Bouvreuril Syenite

The Bouvreuril Syenite, dated to  $1009 \pm 3$  Ma by [12] (Figure 3d), has an octopus-like shape that is easily delimited on an aeromagnetic map. The central part of the body is subcircular in plan, while dikes branch out mainly in an east-west direction. A small satellite intrusion lies to the west of the main body. The Bouvreuril Syenite intrudes the Lacoste Magmatic Suite. The main lithofacies are coarse grained, pink syenite and fine-grained, grey syenite. They are massive and show magma-mingling textures [2]. The main minerals in both syenites are K-feldspar, plagioclase, magnetite, clinopyroxene, biotite, hornblende, and apatite, while ilmenite and pyrite occur as accessory minerals. Dikes are from meters to tens of meters in thickness and consist of megacrystic, pink syenite with 40–50% K-feldspar phenocrysts. East-trending dykes cut the Swamp deformation zone, which affect the Lacoste Magmatic Suite [9,20].

#### 1.2.10. Bourguet Syenite

The Bourguet Syenite, dated to  $1038 +15/-13$  Ma by [2] (Figure 3e), is composed mainly of syenite, along with associated dikes of alkaline syenite, granite, websterite, and gabbro-norite. Syenite is megacrystic and is composed of greyish blue K-feldspar phenocrysts (4–7 cm long), magnetite, biotite, clinopyroxene, apatite while ilmenite and titanite occur as trace minerals. The phenocrysts are perthitic and contain inclusions of apatite and biotite. A subtle preferred orientation of the phenocrysts is of magmatic origin. Alkaline syenite occurs as weakly foliated, fine-grained dikes cutting the principal lithofacies. It contains megacrysts of K-feldspar, along with magnetite, biotite, orthopyroxene, while ilmenite and apatite occur as trace minerals. Granite is pink and coarse grained, and is composed of quartz, plagioclase, and K-feldspar.

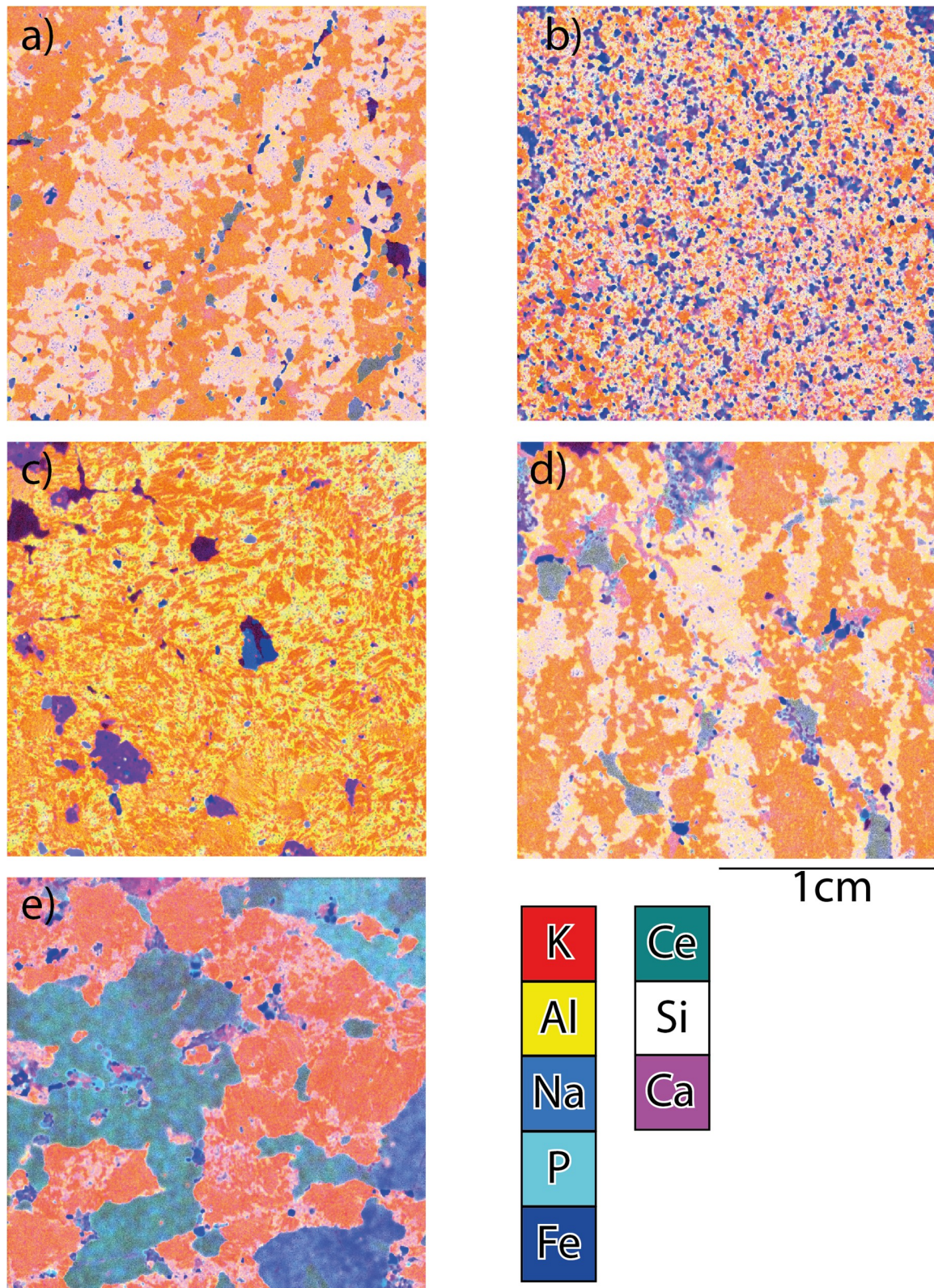


**Figure 3.**  $\mu$ XRF mapping in false color showing the texture and granulometric variation in the different alkaline intrusions. Methodology for mapping can be found in Section 2.3. (a) Wemotaci Intrusion Suite, (b) Rheume Intrusive Suite, (c) Core Syenite, (d) Bouvreuril Syenite, and (e) Bourguet Syenite.

## 2. Materials and Methods

### 2.1. Whole-Rock Geochemistry

Whole-rock geochemical analyses of the syenites were performed by Actlabs (Vancouver, BC, Canada). The major elements were analyzed by inductively coupled plasma–atomic emission spectroscopy (ICP-AES) and trace elements by inductively coupled plasma mass spectrometry (ICP-MS). Analyses were carried out on powdered samples prepared with lithium metaborate or lithium tetraborate. Sample locations are reported as universal transverse Mercator (UTM) coordinates (zone 18, NAD83) in Table S1.

### 2.2. Electron Microprobe Analyses

Electron microprobe analyses were performed using a Cameca computer-controlled SX-100 (Laboratoire de microanalyses, Université Laval; CAMECA, Gennevilliers, France) equipped with a wavelength dispersive spectrometer (WDS). Quantitative analyses of clinopyroxene, plagioclase, hornblende, allanite, carbonate, and apatite were carried out for major and trace elements (La, Ce, Fe, Pr, Nd, Mn, Th, Cr, Co, Ni, Cl, F, P, As, Ba, Sr, Sm, Th, S, Y). Analytical conditions were a voltage of 20 kV and a beam current of 100 nA. Peak counting time was 20 s on the mineral and 10 s for background measurements. The methods for all the elements analysed can be found in Table S3.

### 2.3. $\mu$ XRF

$\mu$ XRF analyses were obtained using a M4 Tornado (Laboratoire de microanalyses, Université Laval; Bruker, Billerica, MA, USA) equipped with a Rh tube with polycapillary optics (50 kV, 300  $\mu$ A) and a spot size of 20  $\mu$ m. The element maps have a size of 1650  $\times$  900 pixels, and spectra were acquired every 30  $\mu$ m with an acquisition time set at 3 msec/pixel. The analyses were performed under a 20  $\mu$ bar vacuum. The  $\mu$ XRF was utilized to identify mineral phases but not to quantify their composition.

### 2.4. U-Pb Methodology

The U-Pb analyses were conducted at GEOTOP, University of Quebec in Montreal. The zircons were separated using disc mill crushing and heavy metal separation with a methylene ( $d = 3.33$ ) iodide heavy liquid. The zircons were selected on the basis of transparency and the absence of cracks. Then, they were analysed by laser ablation inductively coupled plasma mass spectrometry (Thermo Finnigan iCapQ ICP-MS, ThermoFisher, Waltham, MA, USA). A standard (KLO1125) is used to verify the data.

## 3. Results

### 3.1. Whole-Rock Geochemistry

Sixty-four samples were used to characterize the major and trace element compositions of the intrusions. SiO<sub>2</sub> ranges from 45.3% to 70.6%, and Na<sub>2</sub>O + K<sub>2</sub>O from 5.32% to 12.25%. In an SiO<sub>2</sub> vs. K<sub>2</sub>O diagram [21] (Figure 4a) [1], most samples fall in the shoshonite field. However, two samples from the Bourguet Syenite lie in the high-K calc-alkaline field. The compositions of the composite plutons fall in a range of composition including syenodiorite, syenite, and granite fields in a TAS diagram (Figure 4b) [22]. In a calcic to alkaline discrimination diagram (Figure 4c) [23], the syenites fall in the alkaline field. Finally, in a Hf vs Rb/30 vs. 3Ta tertiary discrimination diagram (Figure 4d) [24], the compositions of the composite plutons overlap the fields of volcanic arc granites and within-plate granites. Chondrite-normalized La/Lu ratios range from 4.20 to 93.18, with an average of 23.14.

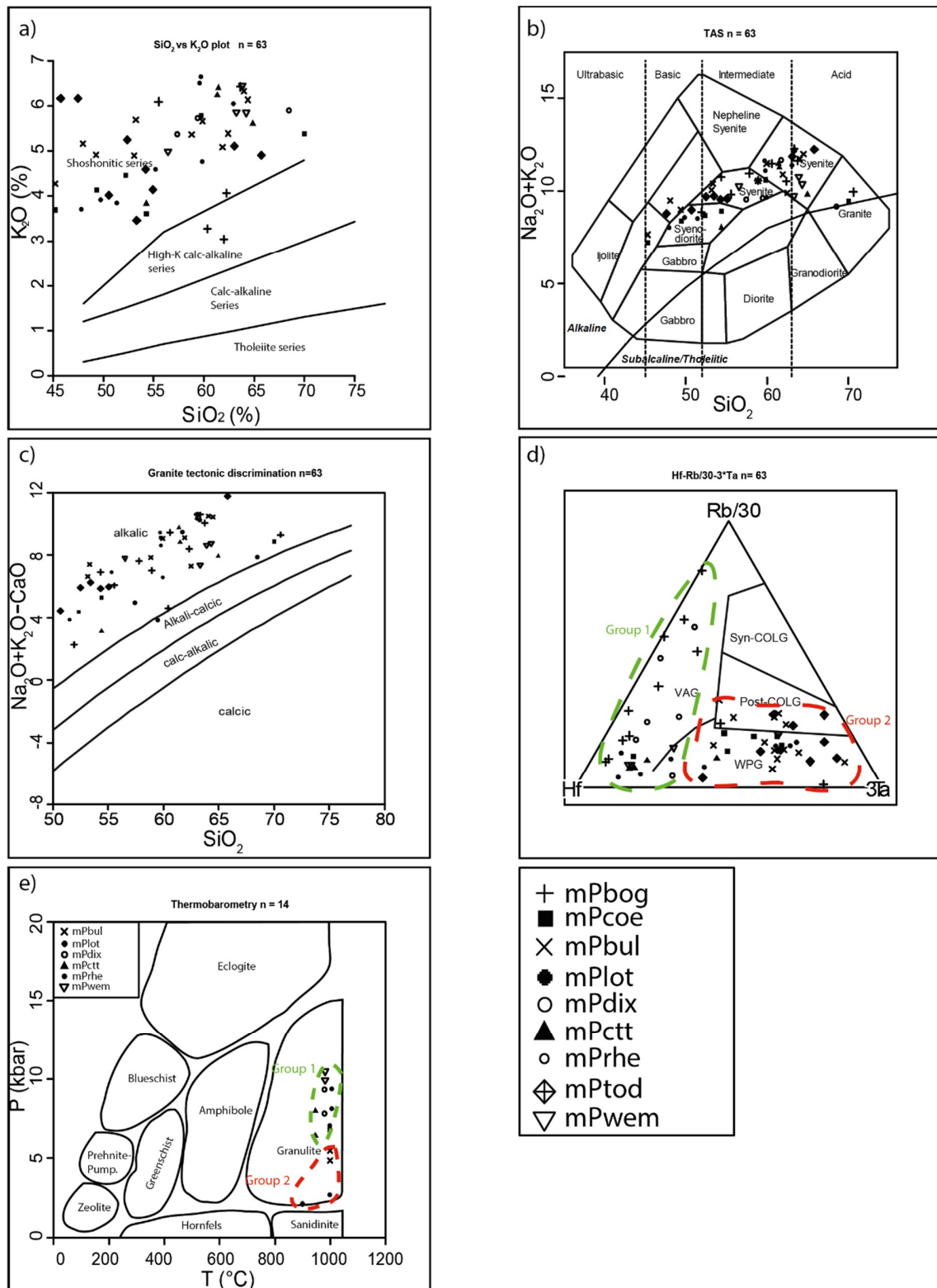


**Figure 4.** Whole-rock geochemistry of the 63 outcrop samples. (a) Affinity  $SiO_2$  vs.  $K_2O$  [21] diagram showing the shoshonitic affinity of the intrusions, (b) Total alkali vs. silice diagram [22] showing the composition range of the intrusions varying from syenodiorite to granite, (c) Granite tectonic discrimination showing the alkaline affinity [23] of the intrusions, (d) Hf vs. Rb/30 vs. 3Ta [24] showing separation of two groups corresponding to different tectono-magmatic systems, (e) thermobarometric results showing the different P-T of the two groups.

### 3.2. Clinopyroxene and Amphibole Thermobarometry

Crystallization temperatures and pressures were calculated for the Bouvreuril, Lortie, Dix Milles, Châteauvert, Rheaume, and Wemotaci syenites using the [25] method. This method uses the clinopyroxene (using the electron microprobe) versus liquid (estimated from whole rock geochemistry) to determine the pressure and temperature of formation of the intrusions. For clinopyroxene-free intrusions, amphibole was used using the [26] method, which uses the amphibole (using the electron microprobe) versus liquid (estimate from whole rock geochemistry) as a geothermometer and plagioclase versus amphibole (using the electron microprobe) aluminium partitioning as a geobarometer. For both methods, the whole-rock composition was considered to represent the composition of the magma from which the clinopyroxene and amphibole crystallized. Both clinopyroxene and amphibole returned syenite crystallization temperatures ranging from 898 to 1005 °C and pressure values ranging from 2.1 to 10.5 kbar (Figure 4e).

### 3.3. Rare Earth Mineralization

Rare-earth minerals are disseminated in various intrusions, but only a few occurrences have high enough values to be classified as “showings” in accordance with an arbitrary value chosen by the MERN (over 1750 ppm REE<sub>total</sub>). The mineralized intrusions include the Bourguet Syenite (sample 14-AM-004A) and the Toad (sample 16-LC-4052B) and Rheaume (sample 16-AE-2126A) intrusive suites. Other mineralized outcrops were mapped, but the REE values are too low to be classified as “showings”. Microscope and electron microprobe work has shown that the minerals hosting rare earths are allanite, parisite, and monazite. Fluorapatite was identified but is REE free. The results of the chemical analyses of these minerals are shown in Table S2.

#### 3.3.1. Parisite

Parisite is a calcium fluorocarbonate containing Ce, La, and Nd. The variety found in the study area is parisite-(Nd). It contains average REE oxide concentrations of 18.4% La<sub>2</sub>O<sub>3</sub>, 28.1% Ce<sub>2</sub>O<sub>3</sub>, and 11.9% Nd<sub>2</sub>O<sub>3</sub>. This mineral forms either prisms or xenomorphic crystals, which are dark grey color and up to 50 µm in diameter (Figure 5a). Parisite is probably an alteration product of allanite.

#### 3.3.2. Allanite-Ce

The allanite group is a member of the epidote supergroup. The variety found in the study area is allanite-(Ce). Its average REE oxide concentrations are 5.5% La<sub>2</sub>O<sub>3</sub>, 10.5% Ce<sub>2</sub>O<sub>3</sub>, and 2.8% Nd<sub>2</sub>O<sub>3</sub>. It does not seem to be associated with any particular rock type or mineral. It is commonly brownish, tabular, idiomorphic, and about 1 mm length (Figure 5b). In places, this mineral is surrounded by radial extension fractures or displays a metamict texture [3]. The allanite has been analysed under an SEM (electron microscope) and the results showed a loss in Ca, Fe and REE. This loss suggests that the REE from allanite could have been used to form parisite and monazite.

#### 3.3.3. Monazite

Monazite is a phosphate containing Ce, La, and Nd. Its average REE oxide concentrations are 23.3% La<sub>2</sub>O<sub>3</sub>, 33.1% Ce<sub>2</sub>O<sub>3</sub>, and 9.8% Nd<sub>2</sub>O<sub>3</sub>. Monazite occurs as small crystals near or within apatite. This mineral is xenomorphic and up to 50 µm in width (Figure 5c). Like parisite, monazite is probably produced during the alteration of allanite.

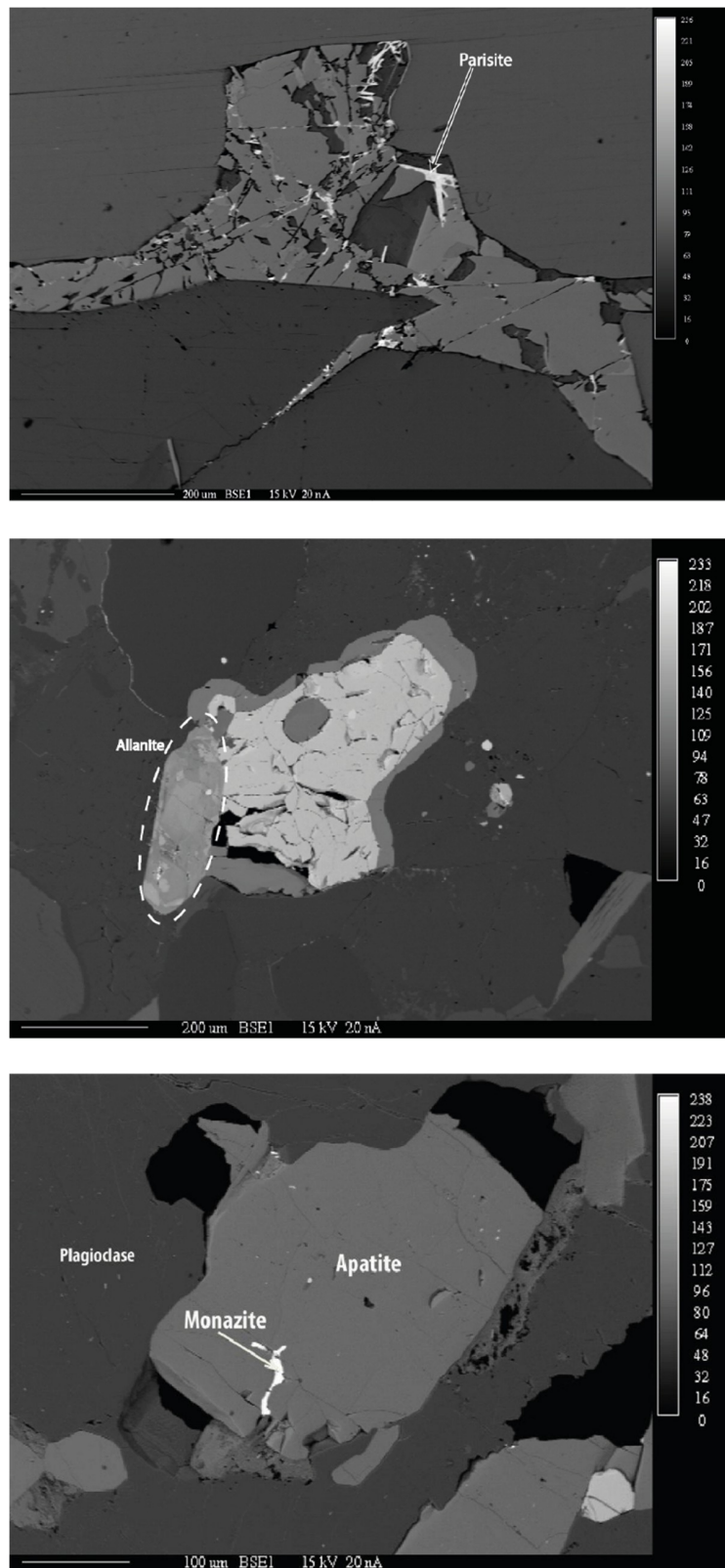


**Figure 5.** Backscattered electron photography of REE-bearing phases in the investigated rocks. (a) represents parisite as a hypidiomorphic crystal which is about 50 μm in diameter near a carbonate mineral, (b) represents the allanite as a large (500 μm) idiomorphic crystal either dissiminated in the matrix or near any other mineral, (c) represents the monazite which is about 100 μm in diameter and always as an inclusion or on the side of the apatite.

### 3.4. Geochronology

#### 3.4.1. Wemotaci Intrusive Suite

##### Zircon Description

Zircons from this syenite (16-GC-1159A) are morphologically homogeneous, hypidiomorphic, colorless in thin section, and contain many inclusions (Figure 6b). The crystals display well-developed prismatic sections, and tips are very short. Cathodoluminescence (CL) images (Figure 6c) show that the core of the crystals are homogeneous and generally bright, and are surrounded by a dark, diffuse band or show lamellar zonation.

##### Analytical Results

Fifty analyses have been conducted by laser ablation. The Th/U ratios vary from 0.39 to 0.81 and show no relation with apparent ages. The analyses return discordant results located slightly above the concordia between 1020 Ma and 1060 Ma (Figure 6a). A linear regression calculation with the lower intersection at the origin showed an upper intersect corresponding to an age of  $1021 \pm 6$  Ma, which is interpreted as a crystallisation age for the syenite.

#### 3.4.2. Rheaume Intrusive Suite

##### Zircon Description

The zircons from this syenite form xenomorphic crystals or very blunt prisms (Figure 6e); they are colorless and up to 500  $\mu\text{m}$  in length. The CL images (Figure 6f) show variable and complex internal structures within single grains.

##### Analytical Results

The results of fifty analyses are distributed on the concordia between 940 Ma and 1060 Ma with a concentration around 1010 Ma to 1020 Ma (Figure 6d). A linear regression gave an upper intersect corresponding to an age of  $985 \pm 9$  Ma. Statistical deconvolution modeling from the  $^{206}\text{Pb}/^{238}\text{U}$  age produced two distinct ages:  $981 \pm 4$  Ma and  $1019 \pm 2$  Ma. The upper intersect age represent less than 25% of the age obtained; consequently, the  $981 \pm 4$  Ma age appears to be too young. For the  $1019 \pm 2$  Ma, the statistical modeling represents 75% of the  $^{206}\text{Pb}/^{238}\text{U}$  ages, which appears more representative of the obtained results. This age is therefore interpreted as the crystallization age of this syenite.

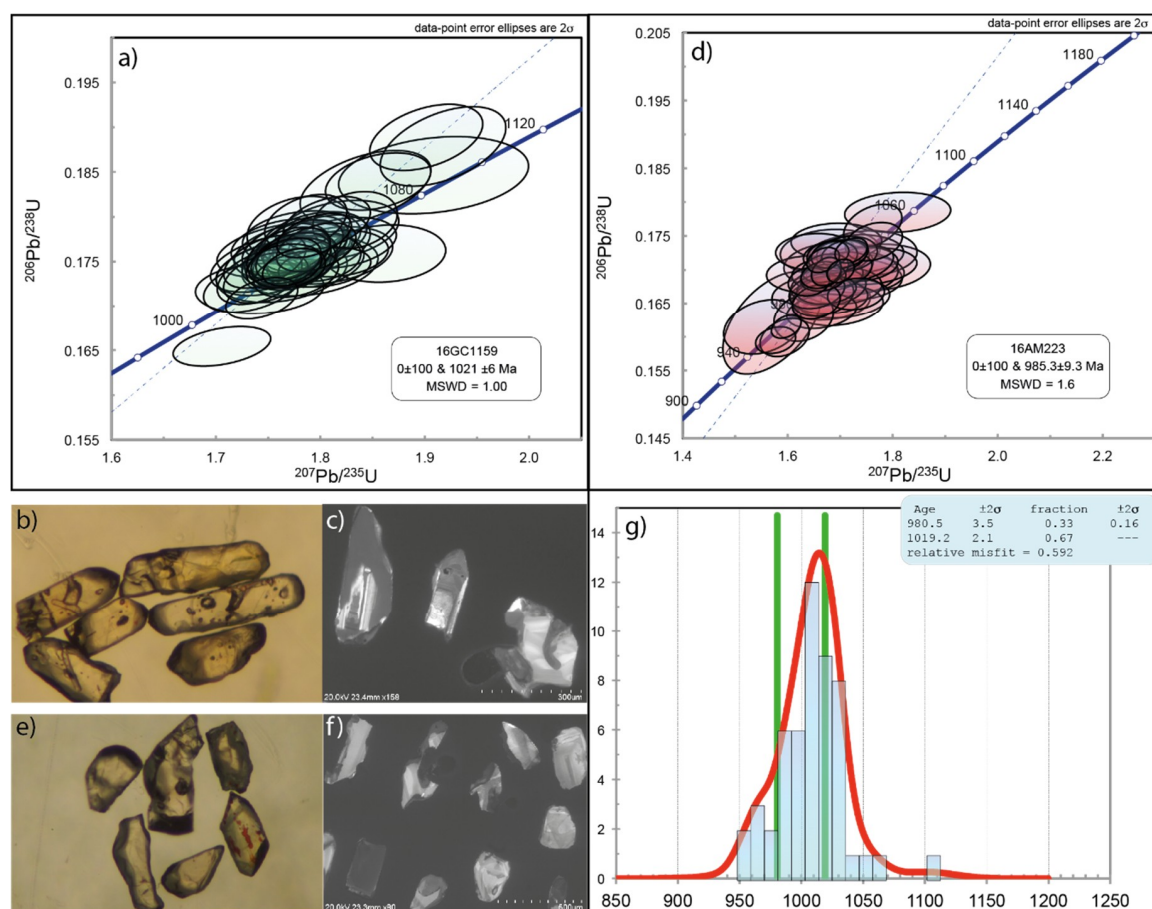


**Figure 6.** Zircon and Concordia diagram (a) Concordia diagram from the zircon of the Wemotaci Intrusive, (b) Zircon from the Wemotaci Intrusive Suite, (c) CL image for the zircon of the Wemotaci Intrusive Suite, (d) Concordia diagram for the zircon of the Rheaume Intrusive Suite, (e) Zircon from the Rheaume intrusive suite, (f) The CL images for the zircon from the Rheaume Intrusive Suite, (g) Statistical deconvolution modeling the results from the zircon of the Rheaume Intrusive Suite.

#### 4. Discussion and Conclusion

The syenites in the Parent region, Canada, were previously studied by [12]. They found that alkaline magmatism in the region occurred between 1040 and 1004 Ma, which is younger than the 1089–1076 Ma age of the Grenville alkaline province as described by many authors [17,27]. The combined results suggest that alkaline magmatism occurred over a period of almost 100 million years in this part of the Grenville Province.

##### 4.1. Geochemical Implications

The data collected indicate that syenitic rocks in the Parent area have a shoshonitic geochemical affinity. They are alkaline, and range from syenitic to granitic in composition. Important differences among the syenites are revealed in the Hf vs. Rb/30 vs 3Ta tectonic discrimination diagram (Figure 4d). Two groups of intrusions are defined, one lying in the volcanic arc granite field and the other in the within-plate granite field. The chondrite-normalized La/Lu ratio shows a general enrichment in LREE in all the syenite of the region. The highest La/Lu ratio does not correspond with the highest enrichment in LREE, which means that there is a weak mineralization in the heavy REE associated with this mineralization.

#### 4.2. Thermobarometric Implications

Thermobarometric results from clinopyroxene-liquid, amphibole-liquid, and Al partitioning methods indicate a crystallization temperature for the syenites ranging from 898 to 1005 °C and pressures ranging from 2 to 10 kbar. On the other hand, this range of pressure (8 kbar) is probably too large for a magmatic event only. Combining the thermobarometric and geochemical results suggests that the volcanic arc syenites had crystallization pressures between 6 and 10 kbar and that the within-plate syenites had crystallization pressures between 2 and 6 kbar (Figure 4e).

#### 4.3. Geological Setting of REEs

Magmatic REE deposits associated with alkaline rocks are important because they have lower grades but higher tonnages than pegmatite. Alkaline intrusions are derived from metasomatically enriched lithospheric mantle [28,29]. The high alkalis and fluorine contents of alkaline magmas increase the solubility of REEs, allowing the crystallization of REE-bearing sorosilicate minerals (allanite) [30]. REEs tend to be associated with the residual magma, which is why they occur in syenites and, more broadly, in associated pegmatites [2,4]. These observations contrast with the interpretations of one recent study [1], who propose that REE-bearing pegmatites result from the melting of underlying supracrustal rocks.

Later in their development, the Haut-Saint-Maurice alkaline intrusions underwent hydrothermal alteration, which resulted in the crystallization of parisite and monazite. Since there is a lack of evidence for widespread hydrothermal alteration, we conclude that the observed alteration was of supergene origin resulting from circulating meteoric waters and that hydrothermal alteration was not responsible for REE remobilization and concentration in the studied intrusions.

Since the REE-bearing syenites have the same geochemistry, composition, ages, and enrichment in light REE, we interpret that the syenitic bodies crystallized from multiple pulses of magma originating from a large magma chamber. The REE-mineralized intrusions probably represent a relatively evolved magma compared to the granites and other intrusion of the region.

#### 4.4. Geodynamic Model

According to many studies [14,31,32], the Grenville orogeny covered the period of 1090–980 Ma. Syn-Grevillian to post-Grevillian intrusions during this period were emplaced in the interior magmatic belt [33]. On the other hand, two studies [12,16] determined three magmatic events during this period. A volcanic arc alkaline magmatic event between 1089 and 1076 Ma in the Mont-Laurier area, a second volcanic arc alkaline magmatic event between 1040 and 1015 Ma in the Haut-Saint-Maurice, and in the same region, a within-plate magmatic event between 1015 and 1000 Ma. Geochemically, our data agree with these results. The REE mineralization associated with syenites tends to be related to the volcanic arc alkalic magmatic event because all the mineralized syenites correspond geochemically and temporally to this event as well. Consequently, in view of our results, the hypothesis of two events occurring during the 1040 to 1000 Ma period seems more suitable. However, as proposed by [16,21] the mantle may have inherited the geochemical signature of volcanic arc magmatism earlier in its history.

1. The first event was an alkaline magmatic event associated with a volcanic arc that occurred between 1040 and 1015 Ma (Figure 7a). During this event, the enriched mantle metasomatism [12] gave rise to a wide range of ultramafic to intermediate alkaline intrusions (glimmerites, syenites, pyroxenites, gabbroites), which are mutually related and show magma-mingling textures. The mantle enrichment resulted in the crystallization of economically interesting REE-bearing minerals (allanite) during this period. Back-arc basin magmatism was probably associated with this event, as indicated by the mafic to ultramafic rocks of the Simoncouche Gabbro. According to [34], this gabbro body formed at a depth of about 18 to 30 km and at a temperature of 937 to 1005 °C.

- The second was an alkalic magmatic event associated with an orogenic collapse that occurred between 1015 and 1000 Ma. This event produced the Labrieville Anorthosite [35], with its associated ultramafic rocks, lamprophyres [36], and alkaline intrusions (syenite and gabbronorite). During this event, there was less REE mineralization. The rocks display a within-plate signature corresponding to extensional magmatism. During this period, there might have been a slab break which provoked an asthenospheric upwelling. This event permitted the crystallisation of mafic to ultramafic rocks as the anorthosite. The emplacement of the Labrieville anorthosite during this period strengthens the anorogenic model. These Haut-Saint-Maurice syenitic intrusions of this period formed at a depth of about 6 to 18 km and at a temperature of 900 to 1000 °C.

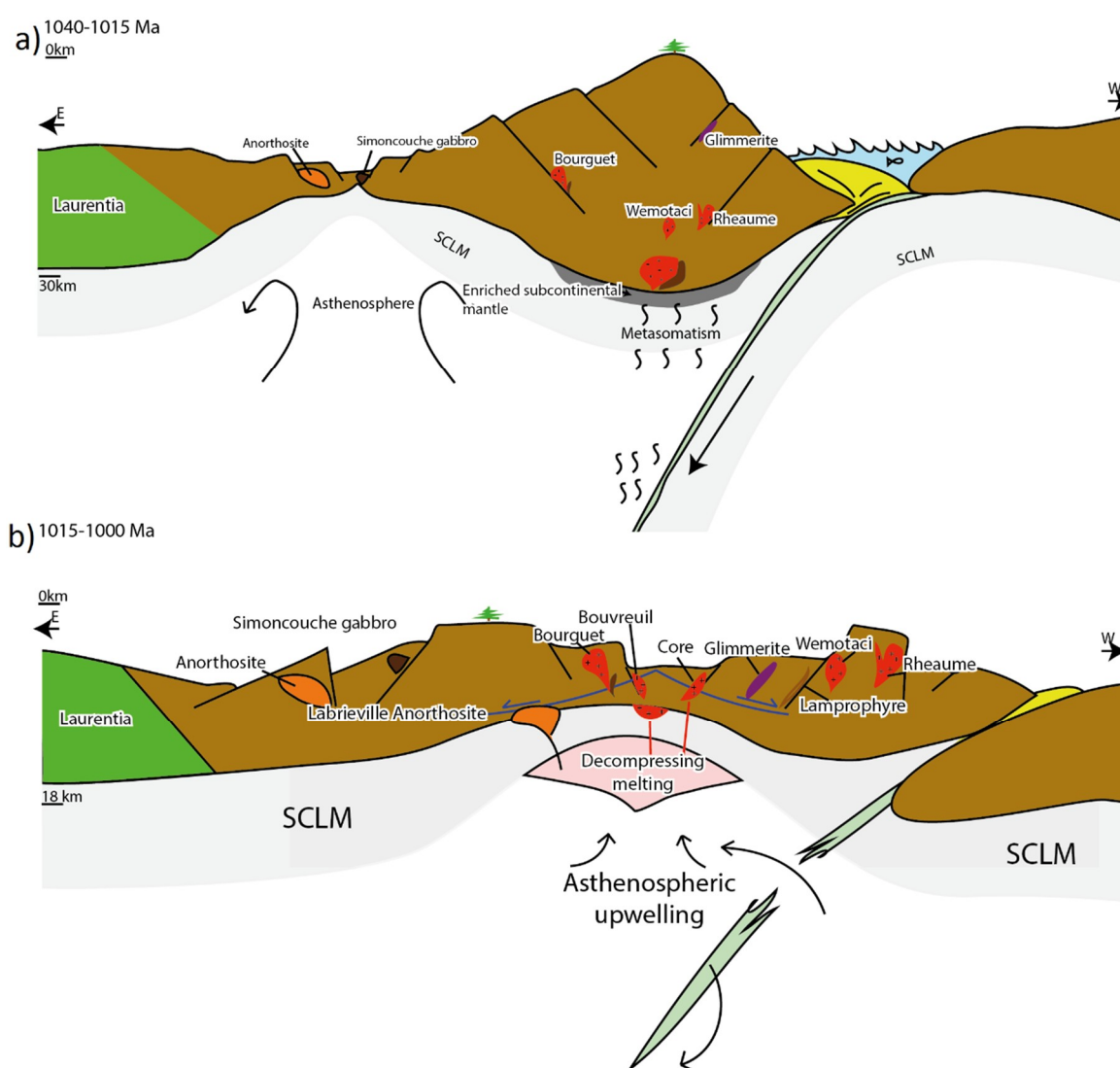


**Figure 7.** Geological model for events between 1040–1015 and 1015–1000 Ma, (a) shows a magmatic event associate with a volcanic arc, (b) shows an alkali magmatic event associated with an orogenic collapse (Simoncouche gabbro [34], Labrieville Anorthosite [35], Lamprophyre [36]).

The interpretation that shoshonitic syenites, associated or not with a parent mafic magma, are related to a subduction zone or to asthenospheric upwelling has been made elsewhere in the world and for different time periods [37–40]. However, in our two-stage model for the period between 1040 and 1000 Ma, we did not take into account the well-accepted continent-continent between

Laurentia and probably Amazonia [41]. During those large orogens, high-grade metamorphic rocks can be exhumed by a single-stage decompression path involving a direct transport of the eclogite-facies rocks into the upper crust [42–44]. Jannin et al. [45] studied high-grade rocks in the Manicouagan region, QC, Canada, and dated two syn-deformation leucosomes which returned two metamorphic ages of  $1002 \pm 2$  and  $986 \pm 4$  Ma. Their results showed that there was a high grade metamorphism during this period. Therefore, the crustal thickening and the continent-continent collision could have happened right after that anorogenic event. Moreover, [46] studied several units in the parautochthone, including Sudbury metadiabase dikes and the River Valley anorthosite and dated the magmatism age using U-Pb titanite and Ar-Ar hornblende. His work suggested that the Grenville Province underwent a shortening of about  $4000 \pm 1000$  km between 1040 and 980 Ma. Those ages are much younger than the 1090 Ma age proposed by [31] and are more concordant with a multi-stage event with a continent-continent collision after 1004 Ma. Therefore, the Grenville Province could have been formed by the collision of many arc terranes followed by a continent-continent collision after 1004 Ma, at least for the Haut-Saint-Maurice part of the Grenville Province. On the other hand, this assumption has not been tested and needs further investigations, including more geochronological and radiogenic isotopes data.

**Supplementary Materials:** The following are available online at <http://www.mdpi.com/2075-163X/8/8/336/s1>, Table S1: Localisation and results of the geochemical date, Table S2: Microprobe analysis, Table S3: Microprobe analysis methods.

**Author Contributions:** Conceptualization, G.C.; Formal Analysis, A.M.; Investigation, G.C.; Data Curation, J.D.; Writing—Original Draft Preparation, G.C.; Writing—Review & Editing, A.M.; Supervision, A.M. and M.C.

**Funding:** This research was funded by Ministère de l'Énergie et des Ressources naturelles grant number 8449-2016-01.

**Acknowledgments:** The authors are grateful to Thomas Clark (MERN) and Héloïse Côté (UQAC) for all the help during the project. The authors also thank Patrice Roy who aided in forwarding of the project. Finally, the authors are also grateful to Marc Choquette (MicroAnalysis Lab, U. Laval) for his technical help and the reviewers from *Minerals* for their time and their recommendations.

## References

1. Turlin, F.; André-Mayer, A.-S.; Moukhsil, A.; Vanderhaeghe, O.; Gervais, F.; Solgadi, F.; Groulier, P.-A.; Pouljol, M. Unusual LREE-rich, peraluminous, monazite- or allanite-bearing pegmatitic granite in the central Grenville Province, Québec. *Ore Geol. Rev.* **2017**, *89*, 627–667. [[CrossRef](#)]
2. Moukhsil, A.; Solgadi, F.; Belkacim, S.; Augland, L.; David, J. *Géologie de la Région de Parent*; Ministère de l'Énergie et des Ressources naturelles: Quebec City, QC, Canada, 2015.
3. Moukhsil, A.; Solgadi, F.; Belkacim, S. *Géologie de la Région de Clova (Partie Ouest du Grenville)*; Ministère de l'Énergie et des Ressources naturelles: Quebec City, QC, Canada, 2016.
4. Moukhsil, A.; Côté, G. *Géologie de la région de Wemotaci*; Ministère de l'Énergie et des Ressources naturelles: Quebec City, QC, Canada, 2017.
5. Currie, K.L.; Van Breemen, O. The origin of rare minerals in the Kipawa Syenite Complex, Western Quebec. *Can. Mineral.* **1996**, *34*, 435–451.
6. Van Breemen, O.; Currie, K.L. Geology and U–Pb geochronology of the Kipawa Syenite Complex—A thrust related alkaline pluton—And adjacent rocks in the Grenville Province of western Quebec. *Can. J. Earth Sci.* **2004**, *41*, 431–455. [[CrossRef](#)]
7. John, E. *An A–Z Guide to the Elements*; Oxford University Press: Oxford, UK, 2001; 538p.
8. Müller, M.A.; Schweizer, D.; Seiler, V. Wealth Effects of Rare Earth Prices and China's Rare Earth Elements Policy. *J. Bus. Ethics* **2016**, *138*, 627–648. [[CrossRef](#)]
9. Nantel, S.; Giroux, F. *Géologie de la Région du Lac Pine*; Ministère de l'Énergie et des Ressources naturelles: Quebec City, QC, Canada, 2004.
10. Corriveau, L.; van Breemen, O. Docking of the Central Metasedimentary Belt to Laurentia in geon 12: Evidence from the 1.17–1.16 Ga Chevreuil intrusive suite and host gneisses, Quebec. *Can. J. Earth Sci.* **2000**, *37*, 253–269. [[CrossRef](#)]

11. Rivers, T.; Culshaw, N.; Hynes, A.; Indares, A.; Jamieson, R. The Grenville Orogen—A post-lithoprobe perspective. In *Tectonic Styles in Canada: The LITHOPROBE Perspective*; Geological Association of Canada: St. John's, NL, Canada, 2012; Volume 49, pp. 97–236.
12. Augland, L.E.; Moukhsil, A.; Solgadi, F. Mantle influence of syn- to late-Grenvillian alkaline magmatism in the Grenville Province: Causes and implications. *Can. J. Earth Sci.* **2017**, *54*, 1–15. [[CrossRef](#)]
13. Rivers, T.; Martignole, J.; Gower, C.F.; Davidson, A. New tectonic divisions of the Grenville Province, southeastern Canadian Shield. *Tectonics* **1989**, *8*, 63–84. [[CrossRef](#)]
14. Gower, C.; Krogh, T. A U-Pb geochronological review of the Proterozoic history of the eastern Grenville Province. *Can. J. Earth Sci.* **2002**, *39*, 795–829. [[CrossRef](#)]
15. Roche, S. L'histoire Tectono-Métamorphique de la Zone de Cisaillement Taureau Orientale et ses Implications Pour L'exhumation de la Croûte Moyenne Dans la Province de Grenville. Master's Thesis, Université du Québec à Montréal, Montréal, QC, Canada, 2014.
16. Corriveau, L. Proterozoic subduction and terrane amalgamation in the southwestern Grenville province, Canada: Evidence from ultrapotassic to shoshonitic plutonism. *Geology* **1990**, *18*, 614–617. [[CrossRef](#)]
17. Currie, K. The alkaline rocks of Canada. *Bull. Geol. Surv. Can.* **1976**, *239*, 228.
18. Blein, O.; LaFlèche, M.R.; Corriveau, L. Geochemistry of the granulitic Bondy gneiss complex: A 1.4 Ga arc in the Central Metasedimentary Belt, Grenville Province, Canada. *Precambrian Res.* **2003**, *120*, 193–217. [[CrossRef](#)]
19. Corriveau, L.; Heaman, L.M.; Marcantonio, F.; van Breemen, O. 1.1 Ga K-rich alkaline plutonism in the SW Grenville Province—U–Pb constraints for the timing of subduction-related magmatism. *Contrib. Mineral. Petrol.* **1990**, *105*, 473–485.
20. Nantel, S.; Giguère, E.; Clark, T. *Geologie de la Région du lac Duplessi*; Ministère de l'Énergie et des Ressources naturelles: Quebec City, QC, Canada, 2003.
21. Peccerillon, A.; Taylor, S.R. Geochemistry of Eocene calc-alkaline volcanic rocks from the Kastamonu area, Northern Turkey. *Contrib. Mineral. Petrol.* **1976**, *58*, 63–81. [[CrossRef](#)]
22. Cox, K.G.; Bell, J.; Pankhurst, R. *The Interpretation of Igneous Rocks*; George Allan & Unwin: Crows Nest, Australia, 1979.
23. Frost, B.R.; Barnes, C.G.; Collins, W.J.; Arculus, R.J.; Ellis, D.J.; Frost, C.D. A Geochemical Classification for Granitic Rocks. *J. Petrol.* **2001**, *42*, 2033–2048. [[CrossRef](#)]
24. Harris, N.B.W.; Pearce, J.A.; Tindle, A.G. Geochemical characteristics of collision-zone magmatism. *Geol. Soc. Lond. Spec. Publ.* **1986**, *19*, 67–81. [[CrossRef](#)]
25. Masotta, M.; Mollo, S.; Freda, C.; Gaeta, M.; Moore, G. Clinopyroxene-liquid thermometers and barometers specific to alkaline differentiated magmas. *Contrib. Mineral. Petrol.* **2013**, *166*, 1545–1561. [[CrossRef](#)]
26. Molina, J.F.; Moreno, J.A.; Castro, A.; Rodríguez, C.; Fershtater, G.B. Calcic amphibole thermobarometry in metamorphic and igneous rocks: New calibrations based on plagioclase/amphibole Al-Si partitioning and amphibole/liquid Mg partitioning. *Lithos* **2015**, *232*, 286–305. [[CrossRef](#)]
27. Corriveau, L.; Gorton, M.P. Coexisting K-rich alkaline and shoshonitic magmatism of arc affinities in the Proterozoic: A reassessment of syenitic stocks in the southwestern Grenville Province. *Contrib. Mineral. Petrol.* **1993**, *113*, 262–279. [[CrossRef](#)]
28. Upton, B.G.J.; Emeleus, C.H.; Heaman, L.M.; Goodenough, K.M.; Finch, A.A. Magmatism of the mid-Proterozoic Gardar Province, South Greenland: Chronology, petrogenesis and geological setting. *Lithos* **2003**, *68*, 43–65. [[CrossRef](#)]
29. Halama, R.; Marks, M.; Brüggmann, G.; Siebel, W.; Wenzel, T.; Markl, G. Crustal contamination of mafic magmas: Evidence from a petrological, geochemical and Sr-Nd-Os-O isotopic study of the Proterozoic Isortoq dike swarm, South Greenland. *Lithos* **2004**, *74*, 199–232. [[CrossRef](#)]
30. Salvi, S.; Williams-Jones, A. Alkaline granite-syenite deposits. *Geol. Assoc. Can.* **2005**, *17*, 315–341.
31. Rivers, T. The Grenville Province as a large hot long-duration collisional orogeny—Insights from the spatial and thermal evolution of its orogenic fronts. *Geol. Soc. Lond. Spec. Publ.* **2009**, *327*, 405–444. [[CrossRef](#)]
32. Hynes, A.; Rivers, T. Protracted continental collision—Evidence from the Grenville Orogen. This article is one of a series of papers published in this Special Issue on the theme Lithoprobe—Parameters, processes, and the evolution of a continent. *Can. J. Earth Sci.* **2010**, *47*, 591–620. [[CrossRef](#)]
33. Rivers, T. Lithotectonic elements of the Grenville Province: Review and tectonic implications. *Precambrian Res.* **1997**, *86*, 117–154. [[CrossRef](#)]

34. Hébert, C.; van Breemen, O. Mesoproterozoic basement of the Lac St. Jean Anorthosite Suite and younger Grenvillian intrusions in the Saguenay region, Québec: Structural relationships and U–Pb geochronology. *Geol. Soc. Am. Mem.* **2004**, *197*, 65–79.
35. Owens, B.E.; Dymek, R.F.; Tucker, R.D.; Brannon, J.C.; Podosek, F.A. Age and radiogenic isotopic composition of a late- to post-tectonic anorthosite in the Grenville Province: The Labrieville massif, Quebec. *Lithos* **1994**, *31*, 189–206. [[CrossRef](#)]
36. Owens, B.E.; Tomascak, P.B. Mesoproterozoic lamprophyres in the Labrieville Massif, Quebec: Clues to the origin of alkalic anorthosites? *Can. J. Earth Sci.* **2002**, *39*, 983–997. [[CrossRef](#)]
37. Štemprok, M.; Seifert, T. An overview of the association between lamprophyric intrusions and rare-metal mineralization. *Mineralogia* **2011**, *42*, 121–162. [[CrossRef](#)]
38. Callegari, E.; Cigolini, C.; Medeot, O.; D’Antonio, M. Petrogenesis of calc-alkaline and shoshonitic post collisional Oligocene volcanics of the Cover Series of the Sesia Zone, Western Italian Alps. *Geodin. Acta* **2012**, *17*, 1–29. [[CrossRef](#)]
39. He, Z.; Xu, X.; Niu, Y. Petrogenesis and tectonic significance of a Mesozoic granite—Syenite—Gabbro association from inland South China. *Lithos* **2010**, *119*, 621–641. [[CrossRef](#)]
40. Wang, K.-L. Geochemical Constraints for the Genesis of Post-collisional Magmatism and the Geodynamic Evolution of the Northern Taiwan Region. *J. Petrol.* **2004**, *45*, 975–1011. [[CrossRef](#)]
41. Li, Z.; Bogdanova, S.; Collins, A.; Davidson, A.; De Waele, B.; Ernst, R.E.; Fitzsimons, I.C.W.; Fuck, R.A.; Gladkochub, D.P.; Jacobs, J.; et al. Assembly, configuration, and break-up history of Rodinia: A synthesis. *Precambrian Res.* **2008**, *160*, 179–210. [[CrossRef](#)]
42. Beaumont, C.; Jamieson, R.A.; Nguyen, M.H.; Lee, B. Himalayan tectonics explained by extrusion of a low-viscosity crustal channel coupled to focused surface denudation. *Nature* **2001**, *414*, 738–742. [[CrossRef](#)] [[PubMed](#)]
43. Vanderhaeghe, O.; Medvedev, S.; Fullsack, P.; Beaumont, C.; Jamieson, R.A. Evolution of orogenic wedges and continental plateaux: Insights from crustal thermal-mechanical models overlying subducting mantle lithosphere. *Geophys. J. Int.* **2003**, *153*, 27–51. [[CrossRef](#)]
44. Jamieson, R.A.; Beaumont, C. On the origin of orogens. *Bull. Geol. Soc. Am.* **2013**, *125*, 1671–1702. [[CrossRef](#)]
45. Jannin, S.; Gervais, F.; Moukhsil, A.; Augland, L.E.; Crowley, J.L. Déformations tardi-grenvilliennes dans la ceinture parautochtone (Province de Grenville centrale): Contraintes géochronologiques par couplage de méthodes U–Pb de haute résolution spatiale et de haute précision. *Can. J. Earth Sci.* **2018**, *55*, 406–435. [[CrossRef](#)]
46. Halls, H.C. Paleomagnetic evidence for ~4000 km of crustal shortening across the 1 Ga Grenville orogen of North America. *Geology* **2015**, *43*, 1051–1054. [[CrossRef](#)]

